Electronic Supplementary Material (ESI) for Physical Chemistry Chemical Physics.

Supporting Information

Unveiling the structure of aqueous magnesium nitrate solutions by combining X-ray diffraction and theoretical calculations

Yunxia Wang,[a, b] Guangguo Wang,[a, b] Daniel T. Bowron,[c] Fayan Zhu,[* a, c] Alex C. Hannon,[*c] Yongquan Zhou,[a] Xing Liu,[d] Guosheng Shi,[a, d, e]

[a] Key Laboratory of Comprehensive and Highly Efficient Utilization of Salt Lake Resources, Qinghai Provincial Key Laboratory of Resources Chemistry of Salt Lakes, Qinghai Institute of Salt Lakes, Chinese Academy of Sciences, Xining 81008, China

[b] University of Chinese Academy of Sciences, Beijing 100049, China

[c] ISIS Facility, STFC, Rutherford Appleton Laboratory, Chilton, Didcot, Oxon OX11 0QX, UK e.

[d] Shanghai Applied Radiation Institute, Shanghai University, Shanghai 200444, China.

[e] Wenzhou Institute, University of Chinese Academy of Sciences, Wenzhou 325001, China

EPSR simulations were carried out at 300 K, and L-J parameters did not change before and after simulation. After 800-2000 steps, the system reached equilibrium state, and the empirical potential values ereq for structural refinement ranges from 5.5 to 9 for the studied systems. The energy, pressure and R-factor at each iteration in the EPSR refinements are shown in the Fig. S1, and the energy variation range after the accumulative process is less than 210 kJ/mol. A full charge and scaled charges 1.5, 1.7 and 1.9 for Mg^{2+} ions and -0.75, -0.85 and -0.95 for NO_3^- ions were used to perform EPSR simulations to effectively include the polarization effect. As shown in Table S4, the coordination number nearly keep constant whether scaled charge was used or not. However, the scaled charge has a major effect on the interaction distance such as Mg-O(W), Mg-N, Mg-O(NO_3), etc. As shown in Tables S4 and S5, the $r_{Mg\text{-}O(W)}$ ~2.10 Å obtained from EPSR using full charge and a scaled charge 1.9 are close to 2.05-2.11 Å in the literatures [1-7]. These EPSR results are also close to our AIMD conclusion. But the $r_{Mg\text{-}O(W)}$ with scaled charges of 1.7 and 1.5 are larger than that of the literatures value 2.11 Å [1-7]. Especially, the $r_{Mg\text{-}O(W)}$ ~2.16 Å with a scaled charge 1.5 cannot be found in previous work. In addition, there is little discrepancy of the second peak in the Mg-O(N) RDFs using full charge and scaled charges (Figs. S2 and S3). For comparison purposes, the RDFs for four atom pairs are also shown in Figs. S2 and S3. There is a small difference between these figures at the same concentration. Based on above, the EPSR simulations using full charge present reasonable results for aqueous $Mg(NO_3)_2$ solutions.

Table S1 Cubic box parameters for the EPSR refinements and AIMD simulations.

WSR	ρ(g/cm^3)	Number density (atoms per Å^3)	EPSR				AIMD			
			n_{Mg}	n_{NO3}	n_{H2O}	Side length /Å	n_{Mg}	n_{NO3}	n_{H2O}	Side length /Å
100	1.0563	0.10082	30	60	3000	45.13	1	2	100	14.5257
60	1.0935	0.10123	50	100	3000	45.36	2	4	120	15.5141
30	1.1770	0.10193	100	200	3000	45.97	4	8	120	15.7204
15	1.3690	0.10245	200	400	3000	47.24	7	14	105	15.4523

Table S2 Lennard-Jones parameters and effective atomic charges used to start the EPSR refinements.

	ε (kJ.mol^{-1})	σ (Å)	Mass	Charge (full)	Charge (1.9)	Charge (1.7)	Charge (1.5)
Mg	0.4593	2.1	24.3050	2.0	1.9	1.7	1.5
N	0.8375	3.9	14.0070	0.8603	0.8173	0.7313	0.6452
ON	0.6490	3.1540	15.9994	-0.6201	0.5891	0.5271	0.4651
OW	0.65000	3.1600	15.9999	-0.8476	-	-	-
OH	0	0	2.0000	0.4238	-	-	-

Table S3 Bond distances and bond angles in the EPSR refinements.

		Bond distances (Å)		Bond angles (°)
NO_3^-	N-O	1.2500	O-N-O	120.0031
		1.2500		120.0031
		1.2500		119.9939
H_2O	OW-HW	0.9574	HW-OW-HW	105.2116
		0.9574		

Table S4 The positions and the average coordination numbers of the atom pairs in aqueous $Mg(NO_3)_2$ solutions obtained from AIMD simulations and EPSR with a full charge and three scaled charges of ions. $r_{(I,\ peak)}$ denotes the peak positions of the first shells. CN_I represents the average coordination numbers of the first shells.

Atom pair	WSR	EPSR		AIMD		EPSR-0.95		EPSR-0.85		EPSR-0.75	
		$r_{(I,peak)}$/Å	CN_I	$r_{(I,peak)}$/Å	CN_I	$r_{(I,peak)}$/Å	CN_I	$r_{(I,peak)}$/Å	CN_I	$r_{(I,peak)}$/Å	CN_I
Mg-O(W)	100	2.10	5.4	2.11	6.0	2.10	5.5	2.13	5.7	2.16	5.6
	60	2.10	5.3	2.09	5.5	2.10	5.4	2.13	5.7	2.16	5.5
	30	2.10	4.9	2.11	4.8	2.10	4.9	2.13	5.1	2.16	5.3
	15	2.15	4.3	2.09	4.6	2.10	4.2	2.13	4.5	2.13	4.8

Mg-O(N)	100	2.10	0.6	-	-	2.13	0.5	2.19	0.3	2.25	0.5
	60	2.10	0.7	2.17	0.5	2.13	0.6	2.19	0.3	2.25	0.5
	30	2.09	1.1	2.17	1.3	2.13	1.1	2.19	0.9	2.25	0.7
	15	2.07	1.7	2.17	1.4	2.13	1.8	2.16	1.5	2.22	1.2
Mg-N	100	3.27	0.6	-	-	3.30	0.5	3.36	0.3	3.42	0.5
	60	3.30	0.7	3.15	0.5	3.30	0.6	3.30	0.3	3.39	0.5
	30	3.28	1.1	3.13	1.2	3.30	1.1	3.36	0.9	3.36	0.7
	15	3.21	1.7	3.15	1.4	3.30	1.8	3.33	1.5	3.36	1.2
N-OW	100	3.59	12.4	3.47	15.7	3.57	11.4	3.60	10.7	3.63	11.1
	60	3.58	12.8	3.47	14.9	3.57	12.4	3.60	12.4	3.60	13.0
	30	3.59	12.4	3.47	14.8	3.57	12.8	3.54	12.5	3.60	12.2
	15	3.56	11.4	3.49	14.0	3.60	12.1	3.60	11.9	3.63	11.9

Table S5 Average hydration shell distances for Mg^{2+}

Solution	Method	$r_{Mg\text{-}O(W)}$/Å	Ref
$Mg(NO_3)_2$	XRD	2.110, 2.104	[1]
$MgCl_2$	ND, MD	2.05, 2.10	[2]
$MgCl_2$	ND, MC	2.10	[3]
Mg Cl_2	QM/MM, MD	2.11	[4]
$MgCl_2$	XRS, SAXS	2.10	[5]
$Mg(NO_3)_2$	XRD	2.066	[6]
$Mg(H_2PO_4)_2$	XRD	2.1	[7]

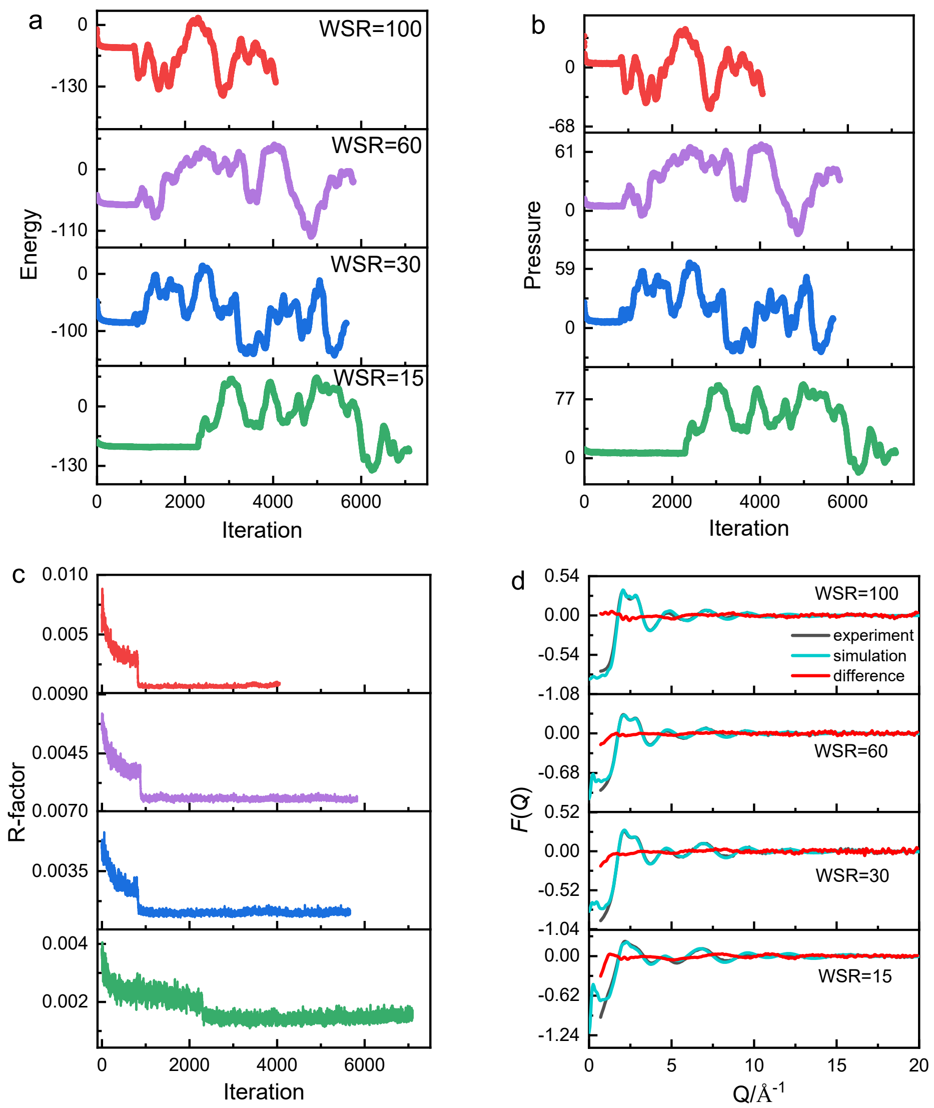

Fig. S1. (a) Energy, (b) pressure and (c) R-factor at each iteration in the EPSR refinements. (d) The difference (red lines) of $F(Q)$ obtained experimentally (black lines) and EPSR simulated (cyan lines) for magnesium nitrate solutions.

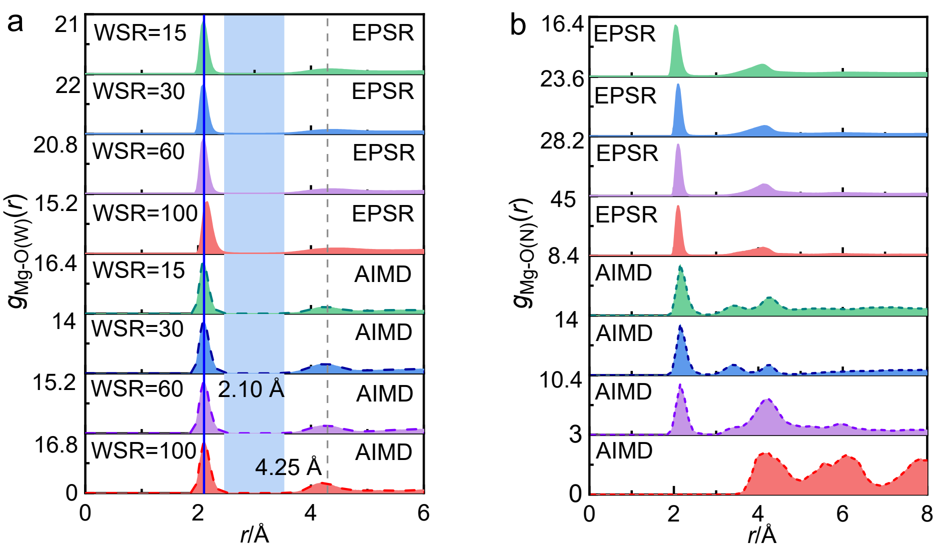

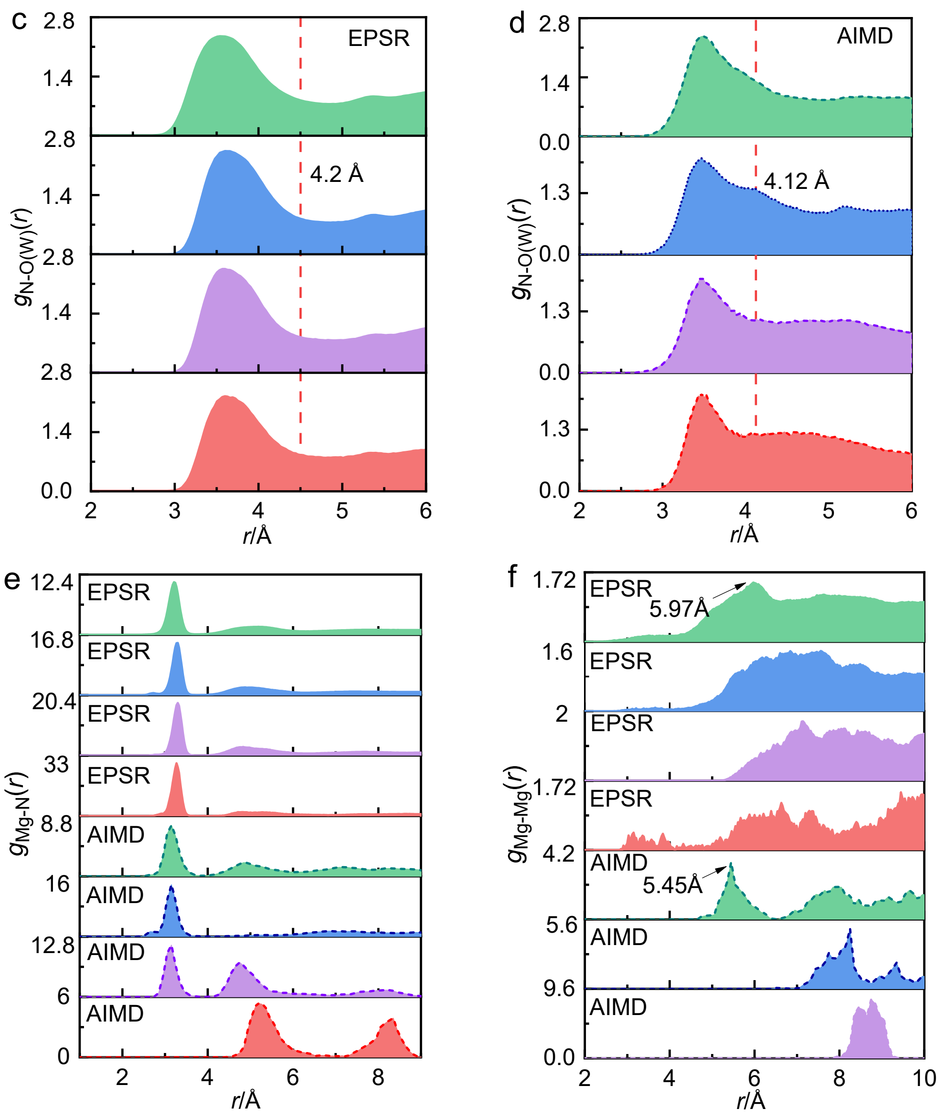

Fig. S2. Pair distribution functions of Mg–O(W) (a), Mg–O(N) (b), N-O(W) (c, d), Mg–N (e) and Mg–Mg (f) at different WSR in $Mg(NO_3)_2$ solutions obtained from EPSR using a full charge and AIMD.

When WSR=15, there are 200 Mg^{2+}, 400 NO_3^-, and 3000 waters in EPSR box, only 7 Mg^{2+}, 14 NO_3^-, and 105 waters in AIMD simulation box (Table S1). From $g_{Mg\text{-}O(N)}(r)$, the first peak is at ~2.1 Å both of EPSR and AIMD results, while the second peak splits at 3.0~5.0 Å of AIMD result (Figs. 5 and S2). It is due to that the EPSR result represents the statistical average, but AIMD result hardly represents the average value because of the little number of ions. But both EPSR and AIMD results confirm that there is qualitatively a broad peak at 3.0~5.0 Å.

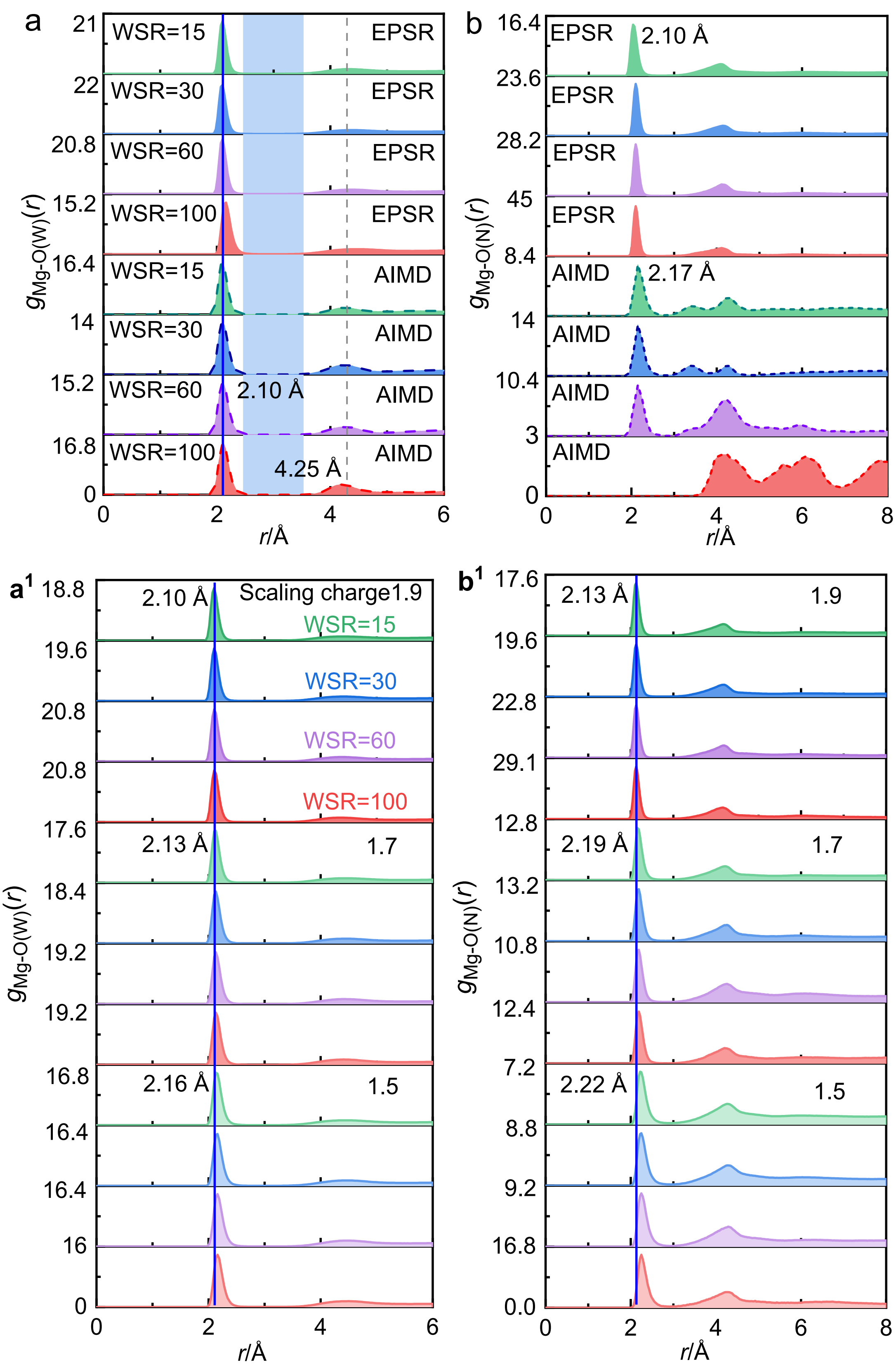

a
b
a1
b1
WSR=15
WSR=30
WSR=60
WSR=100
EPSR
AIMD
2.10 Å
4.25 Å
2.17 Å
2.13 Å
2.16 Å
2.19 Å
2.22 Å
Scaling charge1.9
1.9
1.7
1.5
$g_{Mg\text{-}O(W)}(r)$
$g_{Mg\text{-}O(N)}(r)$
r/Å

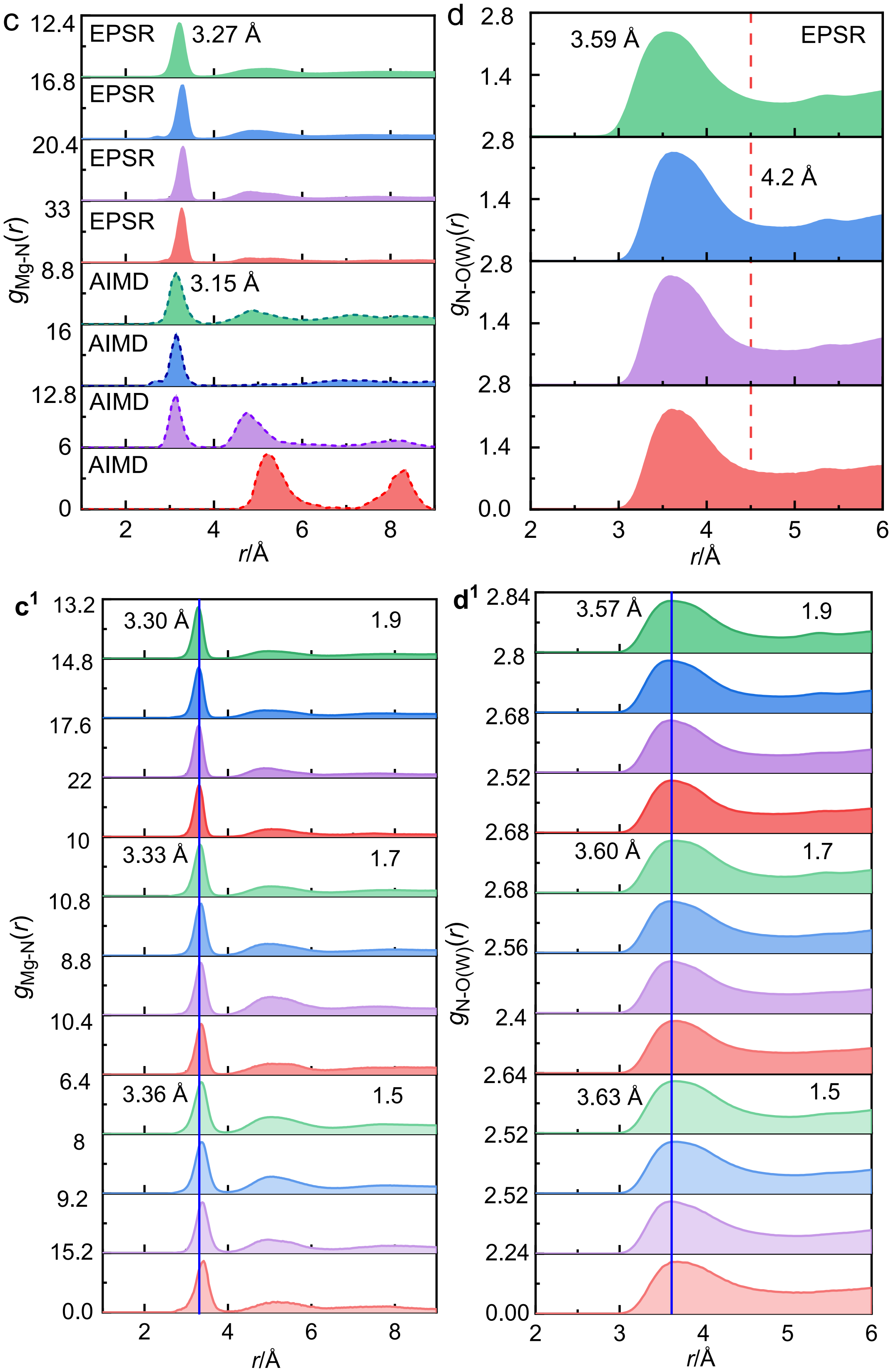

Fig. S3. Pair distribution functions of Mg–O(W), Mg–O(N), Mg–N and N-O(W) at different WSR in $Mg(NO_3)_2$ solutions obtained from EPSR with a full charge (a, b, c, d) and scaled charges of ions (a^1, b^1, c^1, d^1).

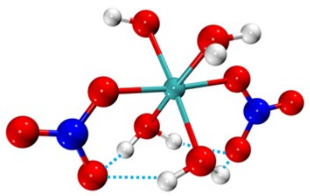

2M1-a

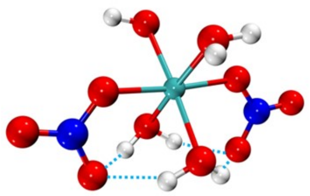

2M1-b

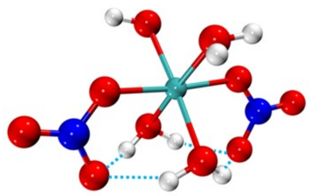

2M1-c

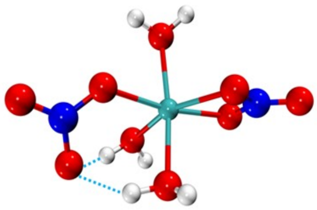

MB-a

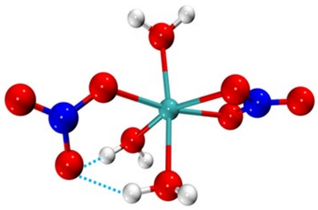

MB-b

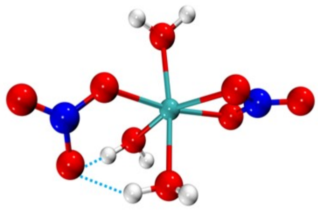

MB-c

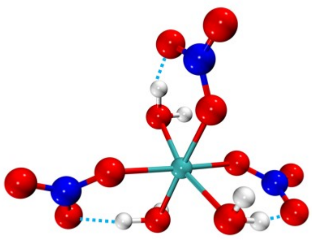

3M-a

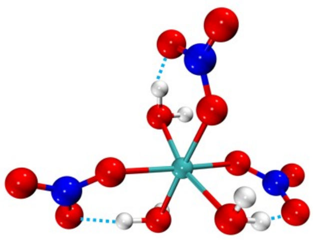

3M-b

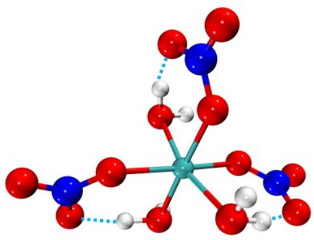

3M-c

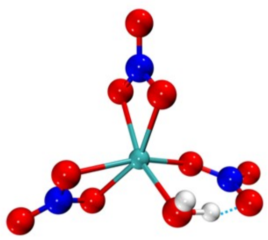

M2B-a

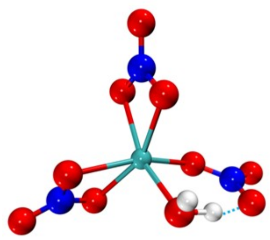

M2B-b

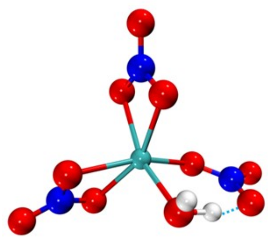

M2B-c

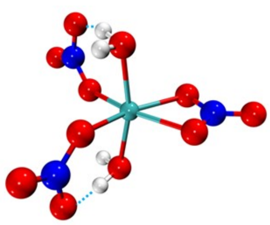

2MB-a

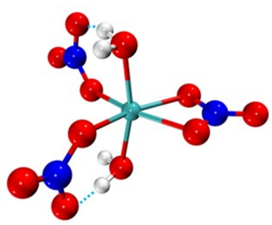

2MB-b

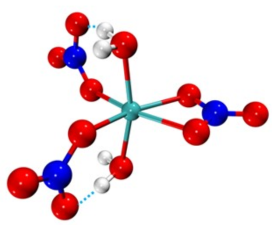

2MB-c

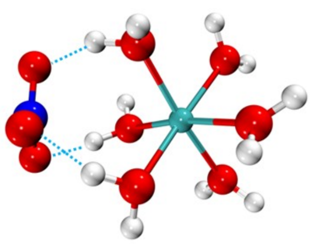

S-a

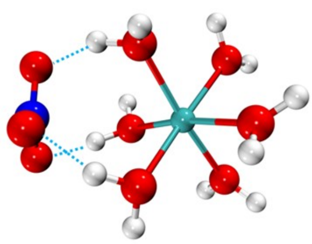

S-b

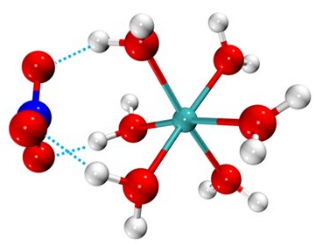

S-c

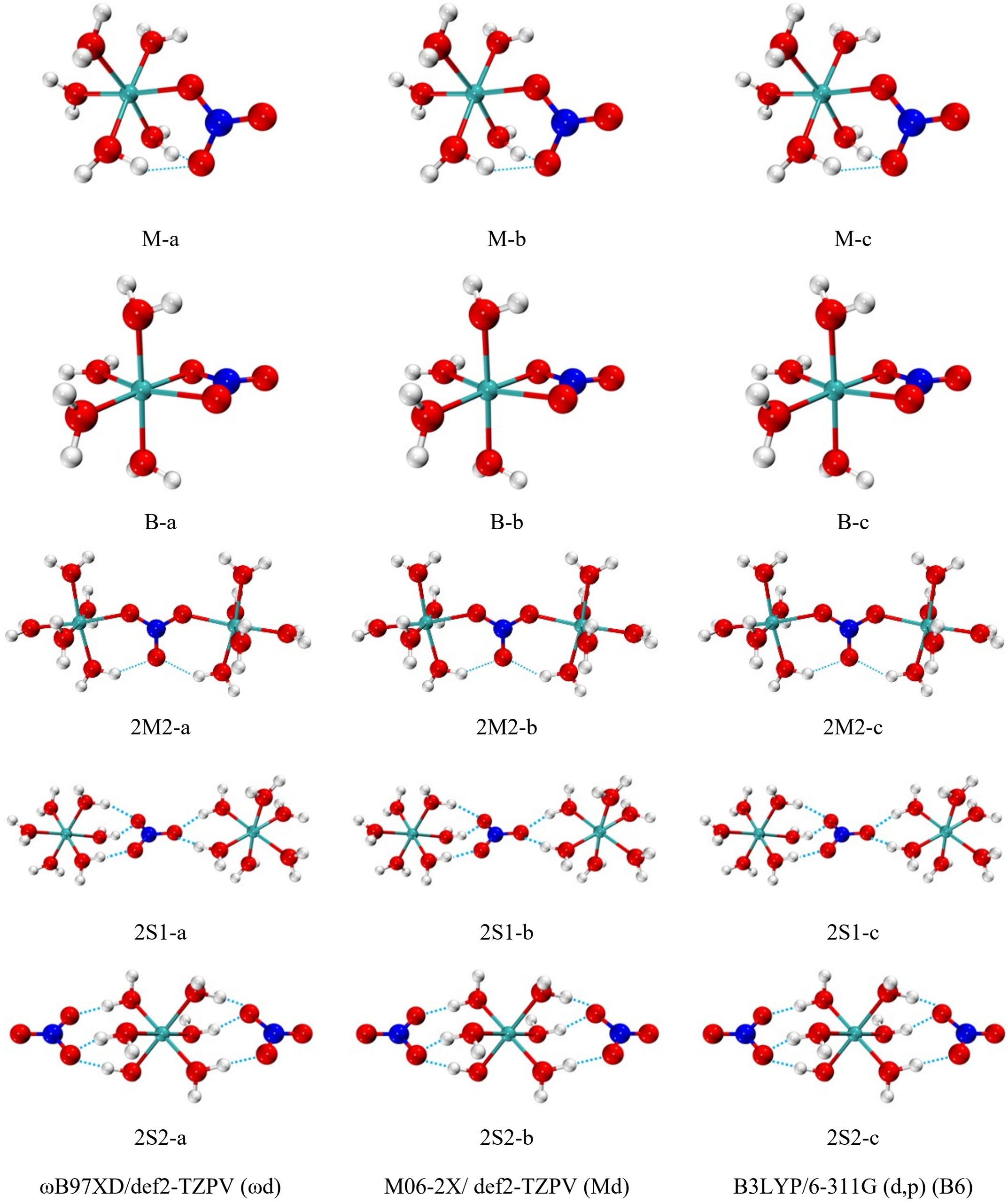

Fig. S4. Ion pairs and multiple ion clusters $[Mg^{2+}{}_{m}(NO_3)^{-}{}_{n}(H_2O)_{q}]$ calculated at three different method/basis sets (abbreviation). The column on the left is calculated at ωB97XD/def2-TZPV (ωd), The middle column is calculated at M06-2X/ def2-TZPV (Md) and the column on the right is calculated at B3LYP/6-311G (d,p) (B6).

Fig. S4 shows that the same structures of $[Mg^{2+}{}_{m}(NO_3)^{-}{}_{n}(H_2O)_{q}]$ were obtained at different method basis sets. Moreover, the bond lengths, vibration frequencies and energies are also listed in Table S6 and S7. These values of the same structure under different method basis sets are close to each other and the variation trend of different structures is basically the same. Therefore, it can be concluded that the method/basis set chosen in this work is appropriate to describe the structures.

Table S6 Atomic distances of ion pairs and multiple ion clusters calculated at different levels.

	$d_{Mg\text{-}ON}$(Å)	$d_{Mg\text{-}N}$(Å)	$d_{Mg\text{-}OW}$(Å)

	ωd	Md	B6		ωd	Md	B6		ωd	Md	B6
2M1	2.039	2.014	2.056	C	2.968	2.943	2.993		2.119	2.075	2.127
	3.094	3.068	3.113	S							
MB	2.095	2.069	2.122	B	2.487	2.458	2.524	B	2.110	2.064	2.113
	2.058	2.026	2.076	M	2.992	2.959	3.020	M			
	3.115	3.083	3.138	S							
3M	2.093	2.06	2.101	C	3.113	3.073	3.155		2.104	2.062	2.109
	3.360	3.319	3.411	S							
M2B	2.122	2.088	2.147	B	2.510	2.471	2.544	B	2.089	2.045	2.096
	2.044	2.015	2.063	M	3.071	3.036	3.110	M			
	3.335	3.297	3.384	S							
2MB	2.116	2.084	2.143	B	2.503	2.466	2.539	B	2.103	2.061	2.105
	2.081	2.046	2.100	M	3.116	3.080	3.147	M			
	3.373	3.338	3.406	S							
S	3.641	3.592	3.691		3.452	3.403	3.501		2.104	2.066	2.108
M	2.020	1.999	2.040	C	2.941	2.921	2.968		2.103	2.061	2.115
	3.038	3.021	2.056	S							
B	2.056	2.035	2.084		2.453	2.429	2.491		2.103	2.059	2.112
2M2	2.153	2.109	2.177	M	3.181	3.135	3.216		2.088	2.049	2.000
	3.481	3.438	3.521	S							
2S2	3.766	3.730	3.807		4.243	4.206	4.296		2.087	2.049	2.100
2S1	3.884	3.854	3.924		4.692	4.659	4.745		2.095	2.055	2.111

ωd, ωB97XD/def2-TZPV; Md, M06-2X/ def2-TZPV; B6, B3LYP/6-311G (d, p).

Table S7 Zero Point energy of ion pairs and multiple ion clusters calculated at different levels.

	Zero Point Energy (a.u.)						
	ωd	Md	B6		ωd	Md	B6
2M1	-1066.6088	-1066.5339	-1066.8177	M	-862.4758	-862.4042	-862.6433
MB	-990.1746	-990.1077	-990.3655	B	-786.0361	-785.9730	-786.1848
3M	-1270.6261	-1270.5443	-1270.8816	2M2	-1444.1906	-1444.0574	-1444.4652
M2B	-1117.7611	-1117.6970	-1117.9770	2S2	-1219.4760	-1219.3794	-1219.7234
2MB	-1194.1965	-1194.1235	-1194.4326	2S1	-1597.0896	-1596.9358	-1597.4022
S	-938.8328	-938.7554	-939.0867				

ωd, ωB97XD/def2-TZPV; Md, M06-2X/ def2-TZPV; B6, B3LYP/6-311G (d, p).

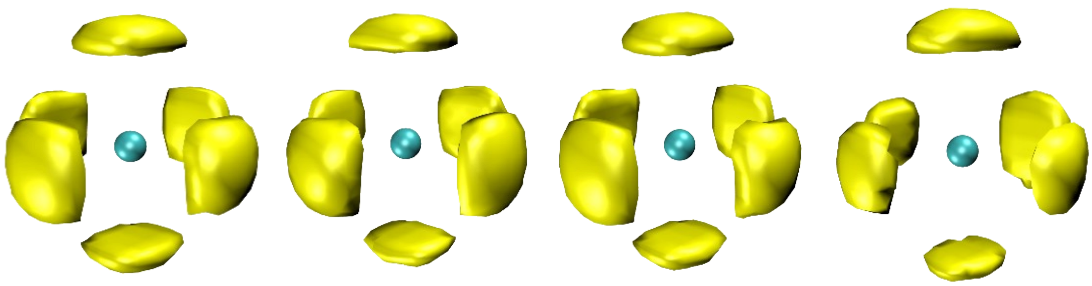

WSR = 100 1.8-3.5 Å 0.6 WSR = 60 1.8-3.5 Å 0.6 WSR = 30 1.8-3.5 Å 0.8 WSR = 15 1.8-3.6 Å 0.8

Fig. S5. SDFs of the distribution of water molecules in the 1.8–3.5 Å range around Mg^{2+}. From left panel to right panel are WSR=100, 60,30,15 respectively. The yellow block represents the first hydration layer of Mg^{2+}, which fractional isosurface level is 0.6 and 0.8 respectively, and the green ball in the middle represents Mg^{2+}.

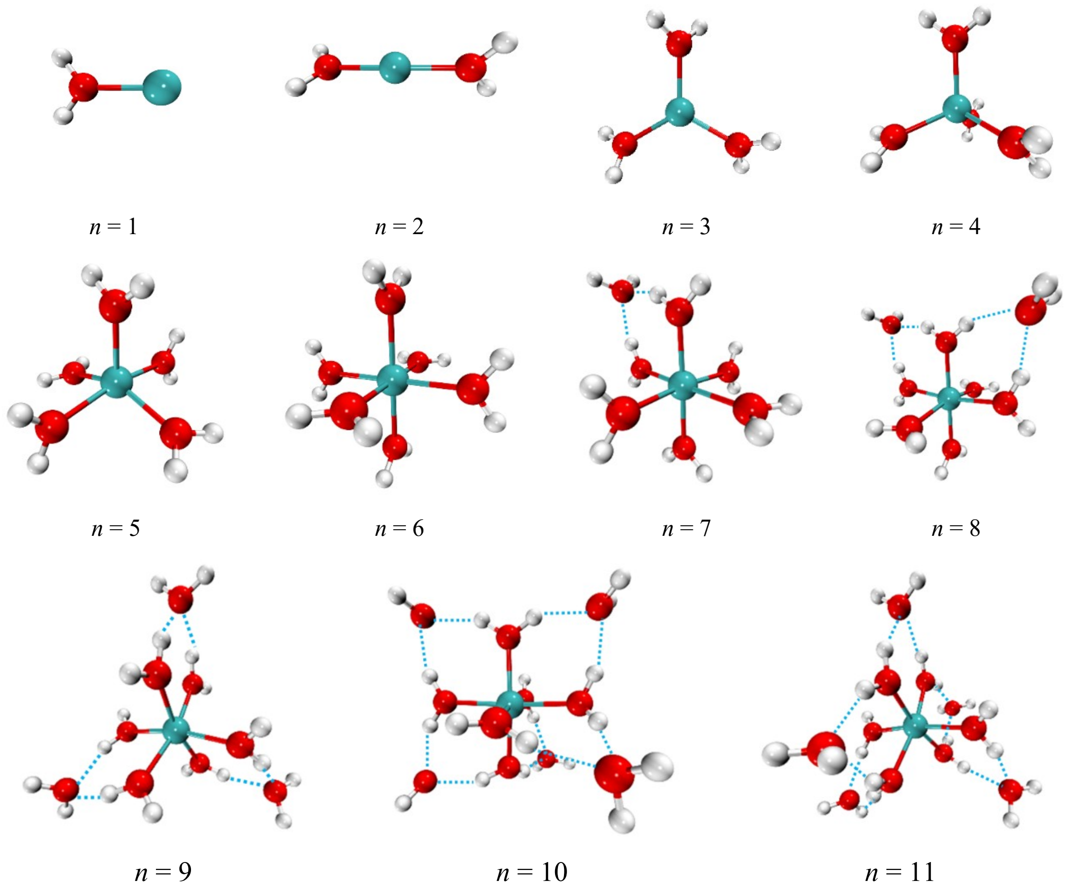

Fig. S6. DFT optimized magnesium hydrate structure.

Table S8 Continuous hydration related energy data of magnesium ions.

N	E_{0b}	E_{Tb}	H_{Tb}	G_{Tb}	ΔE_0	ΔE_T	ΔH_T	ΔG_T
1	310.7794	313.2604	315.7415	287.3284	310.7794	313.2604	315.7415	287.3284
2	296.2473	297.3566	299.8377	268.8056	281.7153	281.4528	283.9339	250.2829
3	274.1383	274.9260	277.4071	244.8552	229.9203	230.0647	232.5458	196.9545
4	253.1861	253.7211	256.2022	222.0221	190.3295	190.1063	192.5874	153.5226
5	229.2575	230.0011	232.4822	195.8197	133.5431	135.1210	137.6021	91.0100

6	211.6323	212.3119	214.7930	176.8055	123.5065	123.8662	126.3473	81.7348
7	194.1386	194.7507	197.2318	159.5889	89.1758	89.3832	91.8643	56.2888
8	181.1281	181.8885	184.3696	145.5631	90.0549	91.8534	94.3345	47.3826
9	170.7434	171.6165	174.0976	134.8849	87.6654	89.4402	91.9213	49.4591
10	160.2173	161.0060	163.4871	124.3433	65.4832	65.5121	67.9932	29.4692
11	151.4549	152.1531	154.6342	115.5147	63.8309	63.6235	66.1046	27.2288

Table S9 The first and second hydration layer radii (r_1 and r_2) and the Mulliken charge of Mg of magnesium hydrate ion.

n	r_1	Mulliken Charge of Mg	n	r_1	r_2	Mulliken Charge of Mg
1	1.9562	1.6699	7	2.1104	3.9048	0.9201
2	1.9724	1.4282	7	2.1040	3.9128	0.9196
3	1.9967	1.2770	9	2.1025	3.9711	0.9066
4	2.0254	1.0717	10	2.1030	3.9571	0.9293
5	2.0744	1.0450	11	2.1011	3.9110	0.8962
6	2.1091	0.9237				

Average energy (E_{0bn}, E_{Tbn}, H_{Tbn}, G_{Tbn}) and successive energy ($\Delta E_{0n,n\text{-}1}$, $\Delta E_{Tn,n\text{-}1}$, $\Delta H_{Tn,n\text{-}1}$, $\Delta G_{Tn,n\text{-}1}$) were copmputed according to

$$E_{0bn} = \left\{E_0(Mg^{2+}) + nE_0(H_2O) - E_0\left[Mg(H_2O)_n{}^{2+}\right]\right\}/n \quad (1)$$

$$E_{Tbn} = \left\{E_T(Mg^{2+}) + nE_T(H_2O) - E_T\left[Mg(H_2O)_n{}^{2+}\right]\right\}/n \quad (2)$$

$$H_{Tbn} = \left\{H_T(Mg^{2+}) + nH_T(H_2O) - H_T\left[Mg(H_2O)_n{}^{2+}\right]\right\}/n \quad (3)$$

$$G_{Tbn} = \left\{G_T(Mg^{2+}) + nG_T(H_2O) - G_T\left[Mg(H_2O)_n{}^{2+}\right]\right\}/nG \quad (4)$$

$$\Delta E_{0n,n-1} = E_0(H_2O) + E_0\left[Mg(H_2O)_{n-1}{}^{2+}\right] - E_0\left[Mg(H_2O)_n{}^{2+}\right] \quad (5)$$

$$\Delta E_{Tn,n-1} = E_T(H_2O) + E_T\left[Mg(H_2O)_{n-1}{}^{2+}\right] - E_T\left[Mg(H_2O)_n{}^{2+}\right] \quad (6)$$

$$\Delta H_{Tn,n-1} = H_T(H_2O) + H_T\left[Mg(H_2O)_{n-1}{}^{2+}\right] - H_T\left[Mg(H_2O)_n{}^{2+}\right] \quad (7)$$

$$\Delta G_{Tn,n-1} = G_T(H_2O) + G_T\left[Mg(H_2O)_{n-1}{}^{2+}\right] - G_T\left[Mg(H_2O)_n{}^{2+}\right] \quad (8)$$

E_0, Sum of electronic and zero-point energies; E_T, Sum of electronic and thermal energies; H_T, Sum of electronic and thermal enthalpies; G_T, Sum of electronic and thermal free energies. all energy data corrected by BSSE.

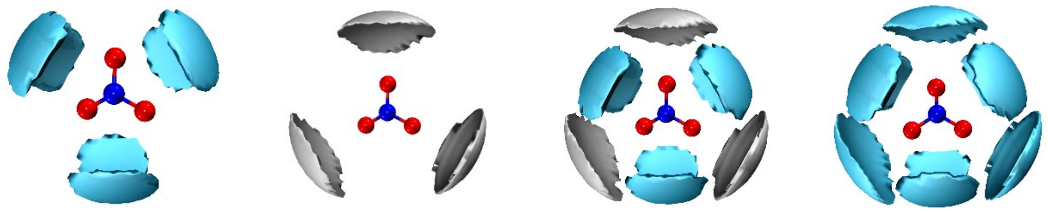

A | B | AB | C

r_{min}-r_{max}: 2.7-3.9 Å | r_{min}-r_{max}: 3.9-4.6 Å | | r_{min}-r_{max}: 2.7-4.6 Å

surfra=0.15 | surfra=0.15 | | surfra=0.2

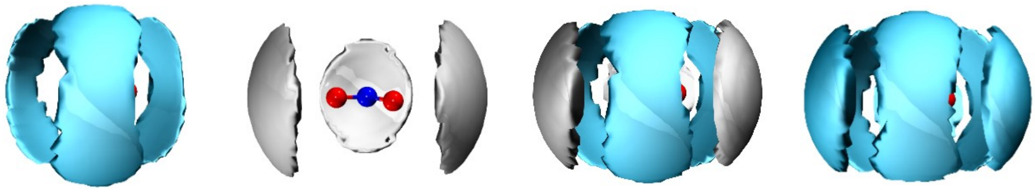

A | B | AB | C

r_{min}-r_{max}: 2.7-3.9 Å | r_{min}-r_{max}: 3.9-4.6 Å | | r_{min}-r_{max}: 2.7-4.6 Å

surfra=0.15 | surfra=0.15 | | surfra=0.2

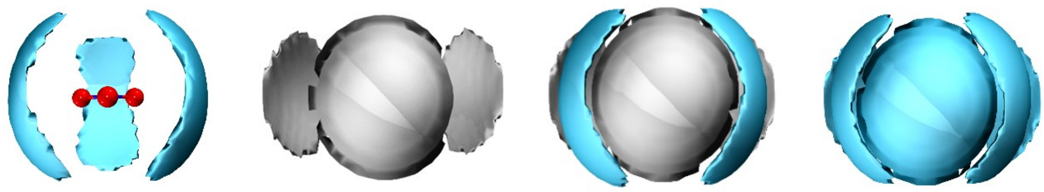

A | B | AB | C

r_{min}-r_{max}: 2.7-3.9 Å | r_{min}-r_{max}: 3.9-4.6 Å | | r_{min}-r_{max}: 2.7-4.6 Å

surfra=0.15 | surfra=0.15 | | surfra=0.2

Fig. S7. The spatial density functions (SDFs) of water molecules around the NO_3^- with a fractional isosurface value of 0.15 at different perspectives. The purple and silver leaf petals represent the probability density of water molecules in the range of 2.7-3.9 Å (A) and 3.9-4.6 Å (B), respectively; gray blue represents the probability density of water molecules in the range of 2.7-4.6 Å (C). Picture AB is the superposition of picture A and picture B. The blue and red balls in the center represent the N and O atoms of NO_3^-, respectively.

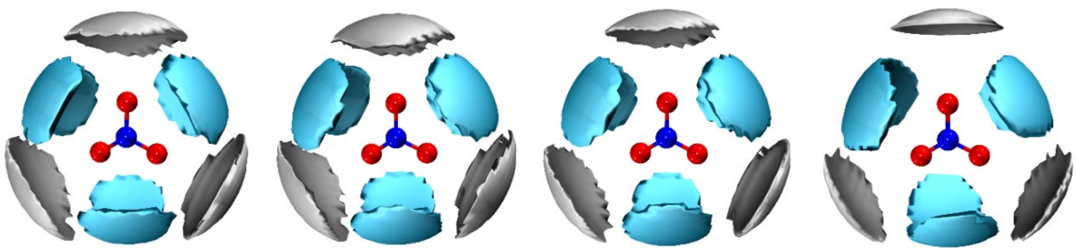

WSR=100 | WSR=60 | WSR=30 | WSR=15

r_{min}-r_{max}: 2.7-3.9 Å (cyan) 3.9-4.6 Å (silver)

Front view

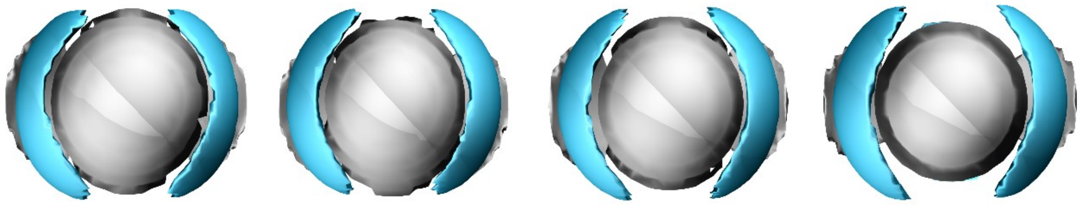

Vertical view

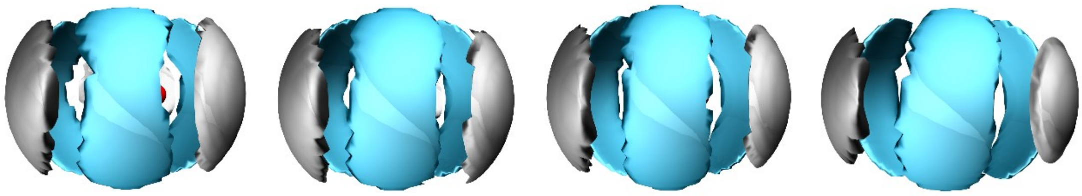

Left view

Fig. S8. The spatial density functions (SDFs) of water molecules around the NO_3^- with a fractional isosurface value of 0.15 at different perspectives. The main, top, and left views of SDFs.

As shown in Figs. S7 and S8, the SDFs of water molecules were calculated within a cutoff distance of 2.6-4.6 Å around the NO_3^-, and truly showed two kinds of hydrated regions as shown in Fig.8. Therefore, the hydrated regions were divided into two kinds: 2.6-3.9 Å as the direct hydration region and 3.9-4.6 Å as the nearest neighbor attachment hydration region. And we distinguish the two kinds of hydration by different colors with a fractional isosurface value of 0.15.

A

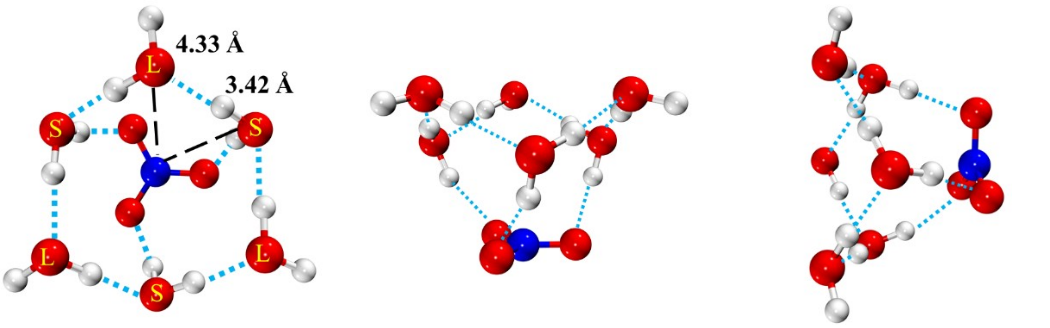

-739.042291 a.u.   0

B

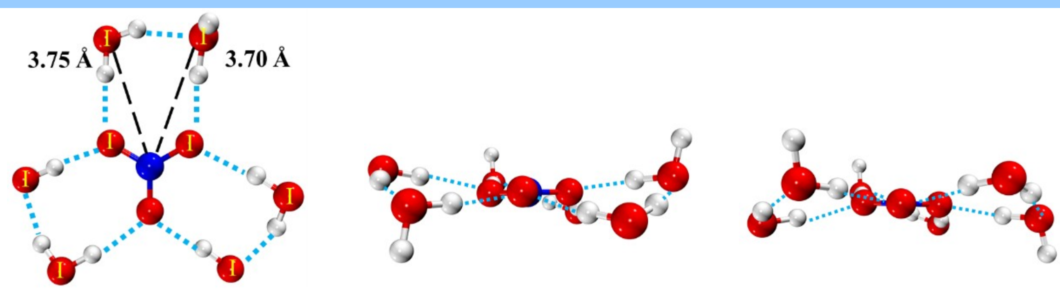

-739.033059 a.u.   24.24 kJ/mol

C

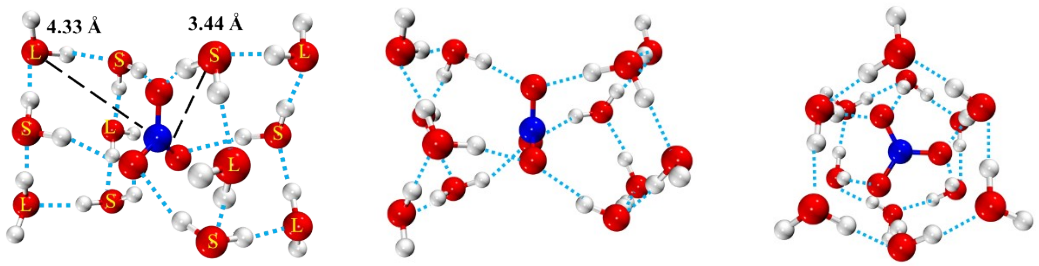

D

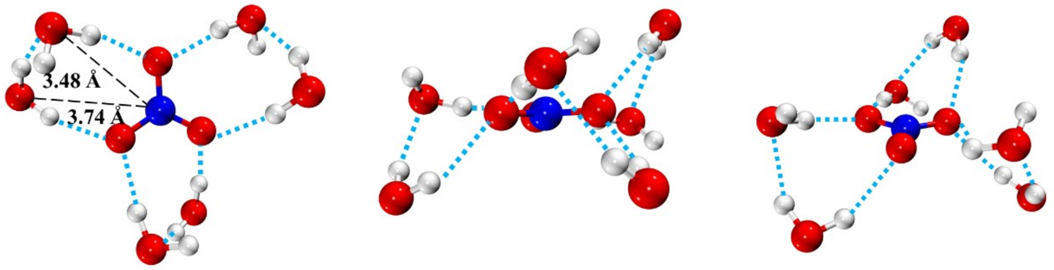

-738.976257 a.u.   173.37 kJ/mol

E

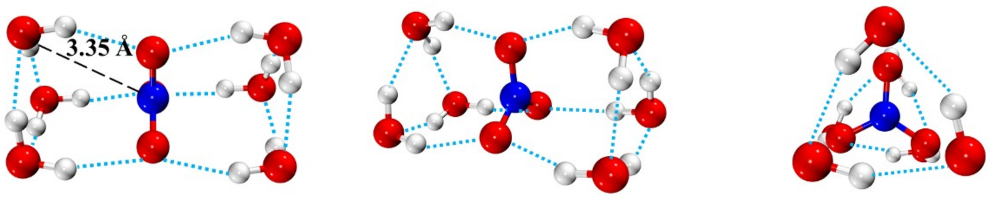

-739.03 a.u.   31.96 kJ/mol

Fig. S9. Multi-angle view of the hydration structure models of [NO_3 $(H_2O)_x^-$] (x = 6, 12) calculated by DFT. The sum of electronic and zero-point energies, and the difference in energy between the isomer and the lowest energy structure were listed below every structure.

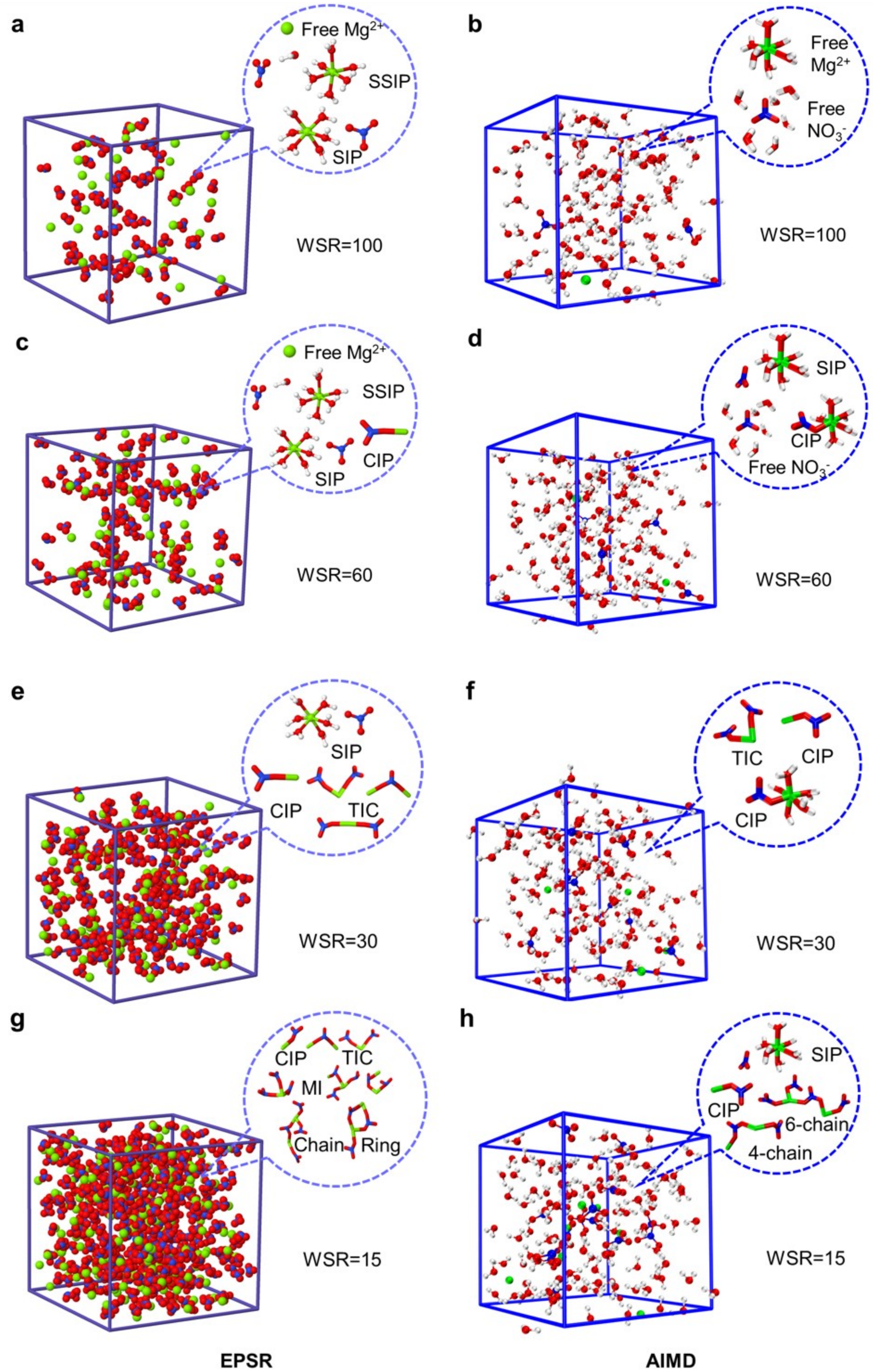

Fig. S10. EPSR (a, c, e, g) and AIMD (b, d, f, h) simulation boxes of magnesium nitrate solutions at different concentrations and the main microscopic species in each box.

References

1 R. Caminiti, G. Licheri, G. Piccaluga and G. Pinna, *Chem. Phys. Lett*, 1979, **61** (1): 45-49.

2 E. Duboué-Dijon, P. E. Mason, H. E. Fischer, P. Jungwirth, *J. Phys. Chem. B*, 2018, **122** (13): 3296-3306.

3 F. Bruni, S. Imberti, R. Mancinelli, M. A. Ricci, *J. Chem. Phys*, 2012, **136** (6): 137-48.

4 S. Riahi, B. Roux, C. N. Rowley. *Can. J. Chem*, 2013, **91** (7): 552-558.

5 I. Waluyo, C. Huang, D. Nordlund, U. Bergmann, T. M. Weiss, L. G. M. Pettersson, A. Nilsson, *J. Chem. Phys*, 2011, **134** (6): 064513.

6 W. Bol, G. J. A. Gerrits, C. L. van Panthaleon van Eck, *J. Appl. Cryst*, 1970, **3**: 486-492.

7 R. Caminiti, *J. Mol. Liq*, 1984, **28** (3): 191-204.